Photodisintegration Studies at HIγS: Addressing the Few and the Many

R. Raut[1],* W. Tornow[2,3], A.P. Tonchev[4], G. Rusev[5], J.H. Kelley[2,6], A.C. Crowell[2,3], M.W. Ahmed[2,7], S.C. Stave[2,8], C. Iliadis[2,9], M. Lugaro[10], J. Buntain[10], R. Schwengner[11], and A. Banu[12]

[1] *UGC-DAE Consortium for Scientific Research, Kolkata Centre, Kolkata 700098, INDIA*
[2] *Triangle Universities Nuclear Laboratory, Durham, North Carolina 27708-0308, USA*
[3] *Duke University, Durham, North Carolina 27708-0308, USA*
[4] *Lawrence Livermore National Laboratory, Livermore, California 94551, USA*
[5] *Los Alamos National Laboratory, Los Alamos, New Mexico 87545, USA*
[6] *North Carolina State University, Raleigh, North Carolina 27695, USA*
[7] *North Carolina Central University, Durham, North Carolina 27707, USA*
[8] *Pacific Northwest National Laboratory, Richland, Washington 99352, USA*
[9] *University of North Carolina at Chapel Hill, Chapel Hill, North Carolina 27695-8202, USA*
[10] *Monash University, Victoria 3800, Australia*
[11] *Institut fur Strahlenphysik, Forschungzentrum, Dresden-Rossendorf, D-01314 Dresden, Germany and*
[12] *James Madison University, Harrisonburg, Virginia 22807, USA*

The High Intensity γ-ray Source (HIγS) of Triangle Universities Nuclear Laboratory (TUNL) is the most intense source of monoenergetic γ-beam in the world. HIγS presents diverse experimental possibilities with wide applications. In the current presentation, we shall be addressing two different experiments on cross-section measuremnts of γ-induced reactions carried out at the HIγS facility. One of them is the measurement of the photodisintegration cross section of ^{4}He$(\gamma,p)^{3}$H and ^{4}He$(\gamma,n)^{3}$He reactions while the other experiment pertains to the cross-section measurements of the ^{86}Kr$(\gamma,n)^{85}$Kr reaction inorder to probe the *s*-process branching point at ^{85}Kr. These measurements highlight the diverse experimental possibilities of the HIγS facility.

1. Introduction

The High Intensity γ-ray Source (HIγS), an experimental facility at the Triangle Universities Nuclear Laboratory (TUNL), is the most intense source of mono-energetic γ-ray beam in the world. HIγS is housed inside the Duke Free Electron Laser Laboratory (DFELL) on the campus of Duke University in the state of North Carolina, USA. The 65000 sq. ft. facility uses the 0.24 - 1.2 GeV Duke Electron Storage Ring as the driver for the γ-ray source. The available γ-beam energies range from 1 to 100 MeV, with small energy spread, desired polarization and high flux ($\sim 10^{8}$ γ/s).

HIγS uses a Free Electron Laser (FEL) for generation of the γ-ray beam. A FEL is based on a relativistic electron bunch in the storage ring as the lasing medium. The γ-ray beam is produced from Compton back-scattering of the FEL photons from the relativistic electron beam in the storage ring. The γ-beam is delivered to the target area through a passive collimation system. The diameter of the collimator essentially determines the energy spread and the profile of the HIγS beam. The γ-beam flux at HIγS can be controlled through a combination of six copper attenuators that can be optionally

*Electronic address: `rraut@alpha.iuc.res.in`

inserted in the path of the HIγS beam. Details of the HIγS facility can be found in Ref. [1].

HIγS presents diverse experimental possibilities in a multitude of domains ranging from few-nucleon physics, low-spin nuclear structure, nuclear astrophysics to measurements pertaining to nuclear applications. Some of these endeavours carried out at HIγS shall be presented herein.

2. Investigation of two-body photodisintegration of ^{4}He at HIγS

The ^{4}He nucleus is the lightest self conjugate nucleus, with a simple closed shell structure. It is often considered as an important link between the classical few-body systems, for example, deuteron, triton, ^{3}He and more complex nuclei. The ^{4}He nucleus provides an ideal testing ground for probing the microscopic two-body and three-body forces. It is expected that the three-nucleon force (3NF) effects would be more important in the four-nucleon (4N) system, with six pairs and four triplets rather than in a three-nucleon (3N) system which has three pairs and only one triplet.

Due to the increased complexity of rigorous 4N calculations as compared to 3N calculations, the theoretical treatment of the photodisintegration of ^{4}He is not as advanced as that of ^{3}He or ^{3}H. Only recently it became possible to calculate the total photo-absorption cross section of ^{4}He [2] with a realistic nucleon-nucleon (NN) potential (Av18) [3] and a 3NF (Urbana IX) [4] using the Lorentz Integral Transform [LIT] method of the Trento group [5]. These calculations reproduce the strong giant dipole resonance peak, but they provide only a 6% reduction in the cross section in this energy regime once the 3NF is turned on. Calculation of the exclusive $^4\text{He}(\gamma,p)^3\text{H}$ and $^4\text{He}(\gamma,n)^3\text{He}$ photodisintegration cross section is even more complex. Theoretical calculations for the ^{4}He(γ,p)^{3}H and $^4\text{He}(\gamma,n)^3\text{He}$ photodisintegration cross section are available from the Trento group [6] in the energy region of interest. Their results were obtained with the semi-realistic central NN potential of the MT I-III type [7], including the Coulomb interaction, and taking into account the full-final state interaction via the LIT method.

There has been a plethora of experimental endeavours on the ^{4}He photodisintegration cross-section (two-body, three-body, total) measurements for many decades. The said measurements have been carried out using both quasimonoenergetic as well as Bremsstrahlung photon beams in the energy range 20-215 MeV. The individual (γ,p) and (γ,n) cross sections have also been determined from the inverse capture reactions. However, the data from all the previous measurements exhibit considerable scattering and barely provides any index to assess the quality of the related theoretical calculations. Of particular concern are the recent results reported by T. Shima *et al.* [8] from the measurements of two-body, three-body and the total photodisintegration cross sections of ^{4}He. The cross-section results of T. Shima *et al.* are around factor of two lower than the theoretical predictions of the Trento group and completely discrepant with respect to all the previous measurements. These results have far reaching consequences. Owing to the analogy between the operators applied in neutrino and γ-induced nuclear reactions, the results of T. Shima *et al.* has a direct impact on the cross sections of the neutrino-nucleus interactions of significance in investigation of core-collapse supernova explosions. Further, the cross-section results of T. Shima *et al.* led to the investigations on the sensitivity of the nonthermal Big Bang Nucleosynthesis (BBN) of the light elements D, T, ^{3}He, ^{4}He, ^{6}Li, ^{7}Li and ^{7}Be to the photodisintegration cross section of ^{4}He. It was established that the change in the ^{4}He photodisintegration cross section has an influence on the nonthermal yields of the light elements D, ^{3}He and ^{4}He, related to the photodisintegration cross sections at low energy ($\sim$ 30 MeV) [9].

In this light, cross-section measurements of ^{4}He(γ, p)^{3}H and ^{4}He(γ, n)^{3}He photodisintegration were undertaken at HIγS with the impetus to provide a conclusive dataset on these reactions [10, 11]. The experimental technique adopted in these measurements at HIγS was that of an active target approach. A high pressure gas scintillator with a mixture of ^{4}He and Xe gas was used as target and detector. Contrary to liquid and plastic scintillators, high pressure gas scintillators are known to have a linear response also for the strongly ionizing particles implying that the amount of light produced is directly proportional to the amount of energy deposited in the gas volume. Consequently, the resulting pulse height is a linear function of the deposited energy irrespective of the identity of the particles (proton, deuteron, triton, ^{3}He, alpha or a Xe recoil) depositing the energy. This feature facilitates easy interpretaion of pulse-height spectra. Except for wall-effects, the efficiency of detection of charged particles is known to be 1.0.

For the present measurements of the ^{4}He(γ, p)^{3}H and ^{4}He(γ, n)^{3}He photodisintegration cross section, a total pressure of 51 atm was used for the ^{4}He and Xe mixture in the high pressure gas scintillator. The Xe in the mixture contributes in enhancing the light output as well as provides stopping power to the protons in the ^{4}He(γ, p)^{3}H cross-secion measurements. The gas mixture was housed in a stainless steel cylinder of wall thickness 1 mm, with a Pyrex glass window at the base coupled to a Hamamatsu H-6410 PMT with a peak sensitivity of 420 nm. The inner surface of the gas housing was coated with MgO as a high-purity reflector material. Diphenylstelbene (DPS) was coated on the MgO layer as well as on the inner surface of the glass window to serve as a wavelength shifter [12].

A. Measurement of ^{4}He(γ, p)^{3}H cross section

The Q-value of the ^{4}He(γ, p)^{3}H reaction is -19.81 MeV. For mono-energetic incident γ-rays of 26 MeV, the total energy deposited by the proton plus triton is 6.2 MeV, while the proton alone has a maximum energy of 5.2 MeV. In pure ^{4}He gas pressurized to 51 atm, the range of those protons would be $\sim$ 4.6 cm, resulting in undesired edge effects in the 5.1 cm diameter stainless steel cylinder, housing the gas. Therefore, depending on the incident γ-ray energy, xenon gas was added at concentrations ranging from 7% to 47%, keeping the total pressure at 51 atm, thus providing the necessary stopping power for the maximum proton range to be less than 1.5 cm. In order to check on photon induced reactions on xenon and the MgO coating on the inner surface of the scintillator vessel, separate measurements were carried out with identical scintillator vessels filled with xenon only.

The absolute γ-ray flux was obtained using the combination of a 10 inch (diameter) x 12 inch (long) NaI detector and the HIγS scintillator paddle system. The paddle system, used for flux measurements at HIγS, is a combination of five thin plastic scintillators with an alumunium radiator in the middle. The working of the paddle system is based on coincident detection of recoil electrons and positrons, generated inside the radiator from the interaction of the incident γ-rays, in the paddles downstream of the radiator. The paddle system was calibrated at reduced γ-ray flux to a NaI detector of known efficiency at individual incident γ-ray energies. In order to eliminate pile-up events in the ^{4}He-Xe gas scintillator and to operate the paddle system in its linear counting-rate range, one of the 8 cm long attenuators made of copper was inserted into the γ-ray beam reducing the γ-ray flux on target to $\sim$ 4 x 10^6 γ/s [10].

Fig. 1 shows typical spectra obtained with incident γ-ray energies of 22.0 MeV for a 47.6 atm ^{4}He - 3.4 atm Xe gas scintillator (a and b). The yield at small pulse heights is dominated by electrons, from the interaction of the incident γ-ray beam with the different components (Xe, ^{4}He etc.) of the gas cell. The enhancement seen at higher pulse heights

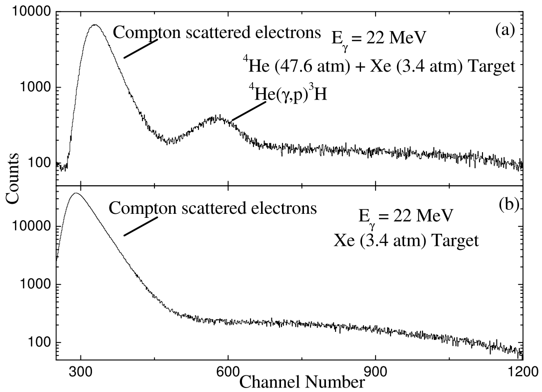

FIG. 1: Spectra for incident γ-energies $E_\gamma = 22.0$ MeV ((a) and (b)) [10].

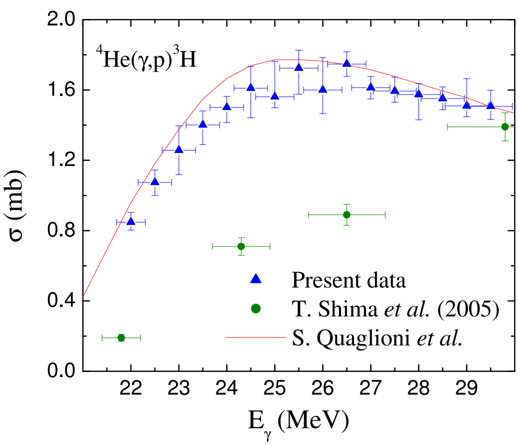

FIG. 2: Present results [10] for the total cross section of the reaction ^{4}He$(\gamma, p)^3$H in comparison to the data of Shima et al. [8] and the theoretical calculation of the Trento group [6].

can be attributed to the protons and tritons from the two-body breakup of ^{4}He. The background due to photon-induced reactions on Xe and the vessel wall extends to even higher pulse heights. The associated pure xenon spectrum indicates a smooth background in the region of interest. The data were corrected for losses of events due to edge effects using Monte-Carlo techniques.

Figure 2 shows the total photodisintegration cross section of the reaction ^{4}He$(\gamma, p)^3$H in comparison to the recent data of Shima *et al.* and the theoretical prediction of the Trento group. The statistical uncertainty in the present data was $\sim 1\%$ or less. The uncertainty in the incident γ-ray flux determination was +2% and -4% with the asymmetry resulting from the fact that the calculated NaI detector efficiency of 0.98 cannot be larger than 1.0. The background subtraction procedure was estimated to contribute an additional uncertainty of about 1 to 10%. The uncertainty associated with determining the helium content in the gas scintillator was 1%. All those uncertainties were added in quadrature, resulting in a total uncertainty of 4 to 13% [10].

The total photodisintegration cross section of the reaction ^{4}He$(\gamma, p)^3$H, from the present work, in the energy range from just above threshold to just below 30 MeV is in fair agreement with the calculations of the Trento group. Applying the about 6% reduction calculated for the total photo-absorption cross section once 3NF effects are included in rigorous 4N calculations using high-precision NN potential models, the current data would be in perfect agreement with the calculation of the Trento group [6]. Therefore, contrary to the findings of Shima et al., present measurements indicate that the theoretical calculations are not only correctly predicting the location of the giant dipole resonance, but in addition, the magnitude of the photodisintegration cross section of the reaction ^{4}He$(\gamma, p)^3$H is very well reproduced, thereby validating the related neutrino-nucleus cross-section calculations.

B. Measurement of ^{4}He$(\gamma, n)^3$He cross section

The experimental approach described in the previous section to measure the ^{4}He$(\gamma, p)^3$H photodisintegration cross section using active target, was extended to measure the ^{4}He$(\gamma, n)^3$He cross section at the peak of the giant dipole resonance. The Q-value for the reaction ^{4}He$(\gamma, n)^3$He reaction is -20.58 MeV. Incident photons with $E_\gamma = 27$ MeV provide helions of energies between 1.0 and

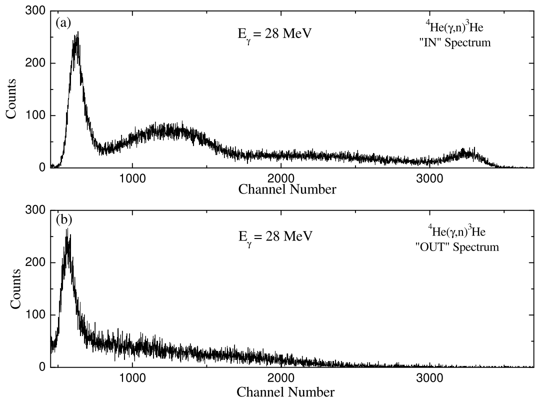

FIG. 3: Pulse-height spectrum of (a) 48.3 atm/2.7 atm ^{4}He/Xe and (b) 2.7 atm Xe gas scintillator obtained with 28.0 MeV mono-energetic photons

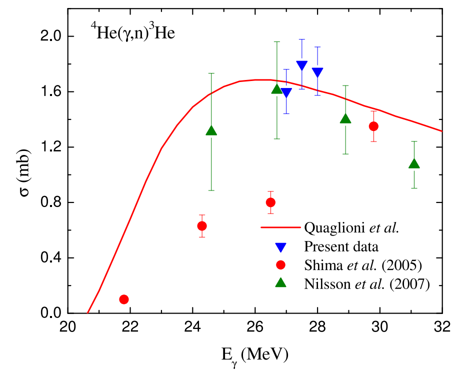

FIG. 4: Cross section results of $^4\text{He}(\gamma,n)^3\text{He}$ reaction from the present work in comparison with the recent literature data and theoretical calculations

2.3 MeV, depending on the emission angle of the undetected neutron. In principle, the pulse-height interval associated with helions should be clearly separated from the summed pulse height of the protons and tritons from the competing reaction $^4\text{He}(\gamma,p)^3\text{H}$, which deposits a total energy of 7.2 MeV for 27 MeV incident photons. However, in standard ^{4}He-Xe gas scintillators, the pulse heights produced by electrons through Compton scattering of the incident γ-rays overlap with those generated by some fraction of the low-energy helions, unless the Xe/^{4}He ratio is kept very low to reduce the stopping power for charged particles. A mixture of 48.3 atm ^{4}He and 2.7 atm Xe was used as target and detector for the $^4\text{He}(\gamma,n)^3\text{He}$ cross-section measurements [11].

Fig. 3 shows the pulse-height spectrum from γ-ray beam incident on the aforesaid ^{4}He (48.3 atm)-Xe (2.7 atm) mixture as well as that from only Xe gas at 2.7 atm. The events stemming from electrons are at the low pulse heights while the broad and symmetric enhancement centered at channel 800 can be attributed to the helions of interest. The broad distribution at large pulse heights is ascribed to the tritons and protons, depositing partial energy in the gas volume, which are also responsible for the saturated events at the very end of the pulse-height distribution. The spectrum obtained with a pure 2.7 atm Xe gas scintillator, indicates the structureless background underneath the region of interest [11].

Fig. 4 illustrates the $^4\text{He}(\gamma,n)^3\text{He}$ cross-section results from the present measurements in comparison to recent data as well as the theoretical calculations of the Trento group. The statistical uncertainty of the present data is below 1%. Similar to the $^4\text{He}(\gamma,p)^3\text{H}$ measurements, the uncertainties in the flux determination is +2% and -4% and that in the He content in the gas is 1%. With the additional uncertainty related to background subtraction in the +6% and -3% range, and all uncertainties added in quadrature, the total uncertainties of the present $^4\text{He}(\gamma,n)^3\text{He}$ cross-section data is in the range +4% to -7%. The present data is in satisfactory agreement with the theoretical calculations as well as the recent experimental results of Nilsson *et al.* [13] and undermines the results of Shima *et al.*. As already discussed in the context of the $^4\text{He}(\gamma,p)^3\text{H}$ measurements, these calculations do not include the three-nucleon forces, including which has shown reduction of 6% in the total photoabsorption cross section of ^{4}He. Extrapolating similar effect in the $^4\text{He}(\gamma,n)^3\text{He}$ cross section would result in good agreement of the present data with the calculations. Calculations with high precion NN potentials and three-nucleon force effects are currently underway [11].

3. Investigation of ^{85}Kr s-Process Branching Point at HIγS

The nucleosynthesis of elements heavier than iron is attributed principally to the slow neutron capture process (*s*-process) and rapid neutron capture process (*r*-process). In addition, 35 proton rich stable isotopes that cannot be produced by either of the aforesaid mechanisms are proposed to be synthesized by the so-called *p*-process, involving a combination of photodisintegration reactions. The designated "slowness" or "rapidness" of the *s* and *r*-processes originate from the relative magnitude of the β-decay lifetime and the neutron capture time scale of the corresponding nuclei. The *s*-process, which operates at low neutron densities ($\sim 10^8$ n/cm^3), is characterized by a long neutron capture times ($\sim$ 1-10 y) compared to the β-decay half-lives of the unstable nuclei. Consequently, the *s*-process closely follow the valley of β-stability on the nuclidic chart. However, certain unstable nuclei on the *s*-process path are characterized by a comparable β-decay half-life and neutron capture timescale. Under such circumstances, the *s*-process bifurcates into the competing neutron capture and β-decay paths and the points of bifurcation are called branching point nuclei. Examples of such branching points include ^{63}Ni, ^{79}Se, ^{85}Kr, ^{147}Nd, ^{153}Gd and ^{185}W. The branching ratio between the β-decay and the neutron capture is extremely sensitive to the prevailing physical conditions in the stellar ambience, characterized by temperature and neutron density. Thus, the branching points serve as an excellent test of the nucleosynthesis models [14]. The branching at ^{85}Kr has profound implications for models of the *s*-process. The operation of the branching point at ^{85}Kr can provide indications on the features of the neutron flux and the conditions in which the neutron sources operate. These features have been used to investigate the *s*-process in asymptotic giant branch (AGB) stars. However, it is a prerequisite of such applications that the ^{85}Kr$(n,\gamma)^{86}$Kr cross section be known accurately. Owing to the short β-decay half-life of the branching point nucleus, it is very difficult to carry out direct neutron capture experiments. Theoretical estimates based on statistical model calculations are sensitive to the choice of parametrizations of level density, γ-ray strength functions and neutron-nucleus optical potential. Neutron capture cross sections on branching point nuclei, in principle, can be derived from probing the (γ,n) photodisintegration cross section of the neighbouring stable nucleus. The impetus is to find a parameter set that reproduces the (γ,n) cross sections and to apply the same set for the reverse (n,γ) reaction to predict the capture cross section on the neighbouring branching point nucleus.

In the present work, the total cross section of the ^{86}Kr$(\gamma,n)^{85}$Kr photoneutron reaction has been investigated [15]. The principal objective was to represent the experimentally measured cross section in statistical model calculations and to use the same parameter set, that best reproduced the data, to predict the neutron capture cross section for the ^{85}Kr *s*-process branching point nucleus. The target consisted of 1012 mg of Kr gas enriched to 99.4% in ^{86}Kr, contained in a stainless steel cell. An empty cell of identical material and dimension was used to subtract the background contribution. The emitted neutrons from the (γ,n) reaction were detected using a 4π assembly of ^{3}He proportional counters, fabricated into a single unit. The ^{86}Kr(γ,n) cross-section measurement was carried out at 24 different γ-energies ranging from threshold (S_n = 9.86 MeV) to 13 MeV. The γ-flux incident on the target was measured using a thin plastic scintillator that was cross-calibrated at seven different γ-energies, between 10.0 and 13.0 MeV. For this purpose, very thin Au-foils of diameter 1.905 cm and thickness 50 μm were positioned

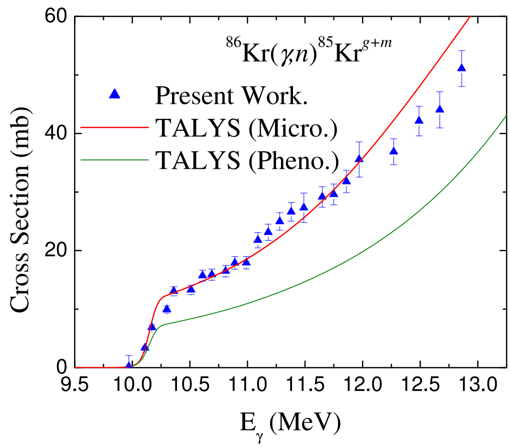

FIG. 5: Measured cross section of the ^{86}Kr$(\gamma, n)^{85}$Kr^{g+m} reaction along with the TALYS calculations using two sets of parameters, phenomenological and microscopic. See text for details.

at the exit end of the γ-beam collimator. The ^{197}Au(γ, n) has been extensively studied and has several advantages of being used as a monitor reaction [18]. In the present work, the cross-section parametrization of Vogt *et al.* [17] was used to calculate the monitor reaction cross section. At each beam energy, consecutive measurements were carried out using the cell filled with ^{86}Kr gas and the empty cell, and the net number of neutrons from the ^{86}Kr(γ, n) reaction was extracted.

The cross-section values from the present measurements are plotted in Fig. 5. The principal sources of uncertainty in the present measurement arise from the efficiency of the ^{3}He proportional counter and the incident γ-flux. Arnold *et al.* [16] have extensively studied the 4π efficiency of the ^{3}He proportional counter and the results were used in the present work for determining the efficiency uncertainties. The uncertainty on the flux determination is principally stemming from the uncertainty on the cross section of the ^{197}Au(γ, n) monitor reaction [17]. The uncertainties were added in quadrature to estimate the total uncertainty on the cross-section values. It should be noted that the statistical uncertainties from the ^{3}He proportional counter or the ^{197}Au monitor reaction were less than 1% at each incident beam energy. Hence, the total uncertainties of the cross-section values were dominated by that on the efficiency of the ^{3}He proportional counter ($\sim$ 3%) and that from the flux estimation using the ^{197}Au(γ, n) reaction ($\sim$ 5%).

Statistical-model calculations were carried out in the present work using the TALYS-1.2 code [19]. The results of these calculations have been plotted along with the experimental cross-section values in Fig. 5. Two different sets of parameters were used in the TALYS calculations. The two sets differed with respect to the choice of models for the nuclear level density and the γ-ray strength function. One set comprised of phenomenological (macroscopic) models, namely the back-shifted Fermi gas model for the nuclear level density and the Lorentzian type E1 strength for the γ-ray strength function. The other set comprised of microscopic models, namely Hartree-Fock-Bogoliubov plus combinatorial method for nuclear level density and Hartree-Fock-Bogoliubov tables for γ-ray strength function. As illustrated in Fig. 5, the TALYS calculations carried out with the microscopic set of parameters are in satisfactory agreement with the experimental results while those with the macroscopic models, though agree at low energies, largely underpredict the cross section for most of the energy range.

As mentioned at the onset, the current work is motivated by the requirement to determine the neutron capture cross section on the *s*-process branching point nucleus ^{85}Kr. Following the satisfactory agreement of the theoretical ^{86}Kr(γ, n) excitation function with the experimental results, the same parameter set was used to calculate the astrophysical reaction rate of the ^{85}Kr(n, γ) neutron-capture reaction. The results are plotted in Fig. 6. This is the first instance where the ^{85}Kr neutron capture rates have been derived based on the experimental data. These rates are currently being applied

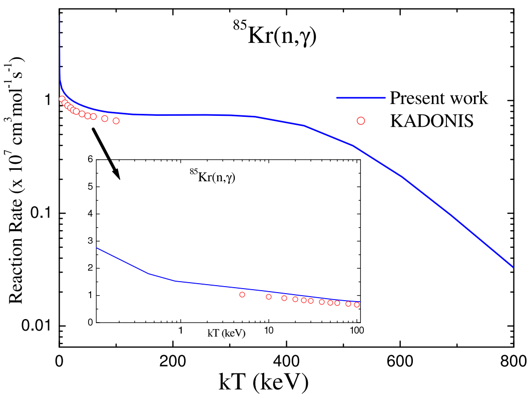

FIG. 6: Astrophysical reaction rates for the ^{85}Kr(n,γ) capture reaction calculated in the present work using TALYS. The parameter set that produced satisfactory agreement of the calculated excitation function with the experimental results for the ^{86}Kr(γ,n) photoneutron reaction was used in the present calculations. The astrophysical rates are compared with those recorded in the KADONIS [20] database.

to astrophysical network calculations and expected to reduce uncertainities on the stellar modelling.

4. Conclusions

This presentation has attempted to discuss cross-section measurements carried out at HIγS, using mono-energetic γ-ray beam. These measurements are of significance in diverse domains of few-nucleon physics and nuclear astrophysics. Measurements on ^{4}He two-body photodisintegration have provided conclusive cross-section data on the ^{4}He$(\gamma,p)^3$H and ^{4}He$(\gamma,n)^3$He reactions and have helped validating the relevant theoretical calculations as well as analogous calculations on neutrino induced nuclear reactions of significance in understanding of core-collapse supernova explosions. The ^{86}Kr$(\gamma,n)^{85}$Kr cross-section measurements have been carried out for the first time and the results have been used to estimate the inverse neutron capture reaction rate on the ^{85}Kr s-process branching point nucleus. The results are of importance in the s-process modelling in AGB stars.

5. Acknowledgements

The work is supported by US DOE grants DE-FG52-09NA29448, DE-PS52-08NA28920 DE-FG02-97ER41033 and DE-FG02-97ER41042. R.R. thanks the Nuclear Physics Group of UGC-DAE CSR, Kolkata Centre, for encouragement and support.

References

[1] H. R. Weller *et al.* Prog. Part. Nucl. Phys. **62**, 257 (2009)
[2] D. Gazit *et al.*, Phys. Rev. Lett. **96**, 112301 (2006)
[3] R. B. Wiringa, V. G. Stoks, R. Schiavilla, Phys. Rev. C **51**, 38 (1995)
[4] B. S. Pudliner *et al.*, Phys. Rev. C **56**, 1720 (1997)
[5] V. D. Efros, W. Leidemann, G. Orlandini, Phys. Lett. B **338**, 130 (1994)
[6] S. Quaglioni *et al.*, Phys. Rev. C **69**, 044002 (2004)
[7] R. A. Malfliet and J. Tjon, Nucl. Phys. A **127**, 161 (1969)
[8] T. Shima *et al.*, Phys. Rev. C **72**, 044004 (2005)
[9] M. Kusakabe *et al.*, Phys. Rev. D **79**, 123513 (2009)
[10] R. Raut *et al.*, Phys. Rev. Lett. **108**, 042502 (2012)
[11] W. Tornow *et al.*, Phys. Rev. C **85**, 061001(R) (2012)
[12] W. Tornow *et al.*, Nucl Instr. Meth. Phys. Res. A**647**, 86 (2011)
[13] B. Nilsson *et al.*, Phys. Rev. C **75**, 014007 (2007)
[14] F. Käppeler, Prog. Part. Nucl. Phys. **43**, 419(1999)
[15] R. Raut *et al.*, Jour. Phys. Conf. Ser. 337, 012048 (2012)
[16] C. W. Arnold *et al.*, Nucl Instr. Meth. Phys. Res. A**647**, 55 (2011)
[17] K. Vogt *et al.*, Nucl. Phy. A **707**, 241(2002)
[18] A. P. Tonchev *et al.*, Phys. Rev. C **82**, 054620 (2010)
[19] A. J. Koning *et al.*, Proc. Int. Conf. Nucl. Data Sci. Tech. 211 (2008)
[20] www.kadonis.org